

Interactions and broken time-reversal symmetry in chaotic quantum dots

Denis Ullmo,^{1,*} Hong Jiang,^{1,2,†} Weitao Yang,² and Harold U. Baranger¹

¹*Department of Physics, Duke University, Durham, North Carolina 27708-0305, USA*

²*Department of Chemistry, Duke University, Durham, North Carolina 27708-0354, USA*

(Received 26 November 2004; published 27 May 2005)

When treating interactions in quantum dots within a random-phase-approximation (RPA)-like approach, time-reversal symmetry plays an important role as higher-order terms—the Cooper series—need to be included when this symmetry is present. Here we consider model quantum dots in a magnetic field weak enough to leave the dynamics of the dot chaotic, but strong enough to break time-reversal symmetry. The ground-state spin and addition energy for dots containing 120–200 electrons are found using local spin-density-functional theory, and we compare the corresponding distributions with those derived from an RPA-like treatment of the interactions. The agreement between the two approaches is very good, significantly better than for analogous calculations in the presence of time-reversal-symmetry. This demonstrates that the discrepancies between the two approaches in the time-reversal symmetric case indeed originate from the Cooper channel, indicating that these higher-order terms might not be properly taken into account in the spin-density-functional calculations.

DOI: 10.1103/PhysRevB.71.201310

PACS number(s): 73.21.La, 73.23.Hk, 05.45.Mt, 71.10.Ay

The impressive progress seen in the recent years in the fabrication and manipulation of semiconductor quantum dots¹ has been associated with a shift in the perspective with which these nanoscopic objects are considered. While the focus used to be on the study of their basic properties, most recent experiments involve them as part of a more complex system in which they play a specific role. Some examples include spin filtering,² charge detection,³ or the manipulation of quantum information.⁴

This stage of maturity of quantum dot physics makes it necessary to go beyond a theoretical understanding of the qualitative properties of these systems, and to also develop good simulation tools which allow one to predict their behavior quantitatively. A natural way to proceed is to rely on density-functional theory.^{5,6} More precisely, since the spin turns out to be an essential degree of freedom, we have in mind a spin-density-functional theory, in the local spin-density approximation (LSDA), where each spin density is taken as an independent variable. The properties of relatively small dots have been investigated in great detail⁷ in this framework, and more recently this approach has been used for significantly larger dots containing several hundreds of electrons.^{8,9}

In this large dot limit, and assuming chaotic dynamics within the dots, it is expected that the fluctuations of experimentally relevant quantities, such as the addition energy or the ground-state spin, should be reliably predicted within a Landau-Fermi-liquid *picture* of the Coulomb interaction and a model of wave functions and eigenenergies based on random matrix theory (RMT) and random plane waves (RPW).^{10–14} (By “fluctuations” we mean the dot-to-dot variation or variation as a function of energy typically seen in mesoscopic systems.¹) We shall below refer to these predictions (somewhat inappropriately) as the “RPA approach” since the Landau-Fermi-liquid picture arises from a random phase approximation (RPA) to the screened Coulomb interaction.^{10,14} Quite unexpectedly, however, for a model chaotic quantum dot the same quantities computed with

LSDA turned out to differ from these theoretical predictions, even at the qualitative level.^{8,9}

This motivated us to introduce a second-order Strutinsky approximation to the LSDA calculations;¹⁵ it was shown to be precise enough to serve as a basis for interpreting the LSDA results. This analysis indicated that the origin of the discrepancies between the LSDA and RPA results arises from two reasons (on which we shall elaborate below): (i) an effective residual interaction which is slightly larger in LSDA; (ii) the absence in LSDA of renormalization of the Cooper channel associated with higher-order terms in the residual interaction. By the Cooper channel we mean the interaction of two electrons following time-reversed paths for which, then, multiple scattering is highly likely.¹⁶

Because the Cooper channel contribution is nonzero only for *time-reversal invariant* systems, a direct implication of the above analysis is that the agreement between LSDA simulation and RPA prediction should be *significantly better* in the presence of a magnetic field strong enough to break time-reversal symmetry. By showing that this prediction actually holds, the goal of this paper is to provide an unambiguous demonstration of the importance of the Cooper channel, and as a consequence, to indicate a possible limitation of the density-functional approach to low-temperature quantum dot properties.

We shall therefore compare in this paper the distribution of addition energies and ground-state spins obtained in two different ways. The first one corresponds to a full-fledged LSDA calculation for a specific model quantum dot. The second is a prediction for a *generic* chaotic system (i.e., not associated with any specific confinement) for which an RPA-like treatment of the interaction is used.

The model quantum dot for the LSDA calculations is confined by the two-dimensional (2D) potential [$\mathbf{r}=(x,y)$],

$$U_{\text{ext}}(\mathbf{r}) = a \left[\frac{x^4}{b} + by^4 - 2\lambda x^2 y^2 + \gamma(x^2 y - y^2 x)|\mathbf{r}| \right], \quad (1)$$

and subjected to the uniform magnetic field $B\hat{z}$. (We use effective atomic units throughout the paper, which, for GaAs

quantum dots with effective electron mass $m^* = 0.067m_e$ and dielectric constant $\epsilon = 12.4$, corresponds to 10.08 meV for energy and 10.95 nm for length.) Here we use $a = 10^{-4}$, which for a particle number in the range [120, 200] gives a parameter $r_s \approx 1.4$ (the ratio between the interaction energy and kinetic energy, formally defined as $r_s = 1/\sqrt{\pi n a_0}$ for 2D bulk systems). The coupling λ between the two oscillators is fixed around 0.6 so that the classical motion within the dot is in the hard chaos regime. Finally, the parameters b and γ eliminate any discrete symmetry. We shall keep $b = \pi/4$ constant, but, to enhance the statistical significance of the various properties studied, we will use the five sets $(\lambda, \gamma) = \{(0.53, 0.2), (0.565, 0.2), (0.6, 0.1), (0.635, 0.15), (0.67, 0.1)\}$.

In the spin-density-functional description, one considers a functional of both spin densities $[n^\alpha(\mathbf{r}), n^\beta(\mathbf{r})]$,

$$\mathcal{F}_{\text{KS}}[n^\alpha, n^\beta] = \mathcal{T}_{\text{KS}}[n^\alpha, n^\beta] + \mathcal{E}_{\text{tot}}[n^\alpha, n^\beta], \quad (2)$$

where $\sigma = \alpha, \beta$ corresponds to majority or minority spins, respectively. The second term is an explicit functional of the densities,

$$\begin{aligned} \mathcal{E}_{\text{tot}}[n^\alpha, n^\beta] \equiv & \int d\mathbf{r} n(\mathbf{r}) U_{\text{ext}}(\mathbf{r}) + \frac{e^2}{2} \int d\mathbf{r} d\mathbf{r}' \frac{n(\mathbf{r})n(\mathbf{r}')}{|\mathbf{r} - \mathbf{r}'|} \\ & + \mathcal{E}_{\text{xc}}[n^\alpha, n^\beta], \end{aligned} \quad (3)$$

where $n(\mathbf{r}) = n^\alpha(\mathbf{r}) + n^\beta(\mathbf{r})$, $U_{\text{ext}}(\mathbf{r})$ is the exterior confining potential Eq. (1), and we use the Tanatar-Ceperley parametrization of the exchange-correlation term $\mathcal{E}_{\text{xc}}[n^\alpha, n^\beta]$ (Refs. 17 and 18).

The kinetic-energy term $\mathcal{T}_{\text{KS}}[n^\alpha, n^\beta]$, on the other hand, is expressed in terms of a set of auxiliary orthonormal functions $\psi_i^{\alpha, \beta}$ ($i = 1, \dots, N^{\alpha, \beta}$) as

$$\mathcal{T}_{\text{KS}}[n^\alpha, n^\beta] = \sum_{\substack{\sigma=\alpha, \beta \\ i=1, N_\sigma}} \int \psi_i^{\sigma*}(\mathbf{r}) \frac{[\mathbf{p} - (e/c)\mathbf{A}(\mathbf{r})]^2}{2m} \psi_i^\sigma(\mathbf{r}) d\mathbf{r}, \quad (4)$$

with $\mathbf{A}(\mathbf{r})$ the vector potential generating the magnetic field and $n^\sigma(\mathbf{r}) \equiv \sum_{i=1}^{N_\sigma} |\psi_i^\sigma(\mathbf{r})|^2$.

The LSDA energy for a given value of the total number of particles $N = N^\alpha + N^\beta$ and spin $S = (N^\alpha - N^\beta)/2$ is obtained by minimizing the functional Eq. (2) under the constraints $\int d\mathbf{r} n^{\alpha, \beta}(\mathbf{r}) = N^{\alpha, \beta}$. The ground-state energy for a given N is then obtained by picking the spin S with lowest energy. The details of the practical implementation of these calculations can be found in Ref. 19.

Already quite good approximations of the densities $n_{\text{TF}}^{\alpha, \beta}(\mathbf{r})$ are obtained via the Thomas-Fermi approximation (see, e.g., Fig. 2 in Ref. 15), which amounts to replacing the Kohn-Sham kinetic energy, Eq. (4), by the explicit density functional

$$\mathcal{T}_{\text{TF}}[n^\alpha, n^\beta] = \frac{1}{2N(0)} \int d\mathbf{r} [n^\alpha(\mathbf{r})^2 + n^\beta(\mathbf{r})^2] \quad (5)$$

(valid in 2D) with $N(0) = m/\pi\hbar^2$ the two-dimensional density of states. Once the Thomas-Fermi calculation has been performed (see Ref. 20 for the practical implementation), the

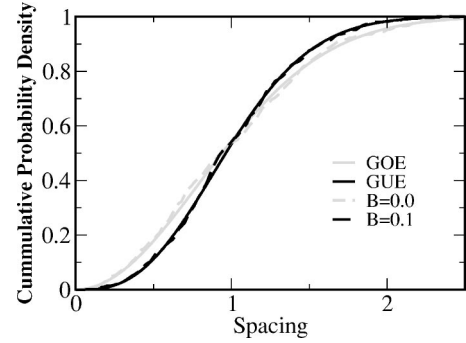


FIG. 1. Cumulative density of nearest-neighbor level spacing for the effective Hamiltonian derived from the Thomas-Fermi approximation at $B=0$ T (dashed gray) and $B=0.15$ T (dashed black). The solid lines are the corresponding Wigner surmise distributions for the orthogonal (gray) and unitary (dark) Gaussian ensembles.

(spin-dependent) one-particle effective Hamiltonian

$$H_{\text{TF}}^{\alpha, \beta} = [\mathbf{p} - (e/c)\mathbf{A}(\mathbf{r})]^2/2m + U_{\text{TF}}^{\alpha, \beta}(\mathbf{r}), \quad (6)$$

defined in terms of the Thomas-Fermi self-consistent potential

$$U_{\text{TF}}^{\alpha, \beta}(\mathbf{r}) = \frac{\delta \mathcal{E}_{\text{tot}}}{\delta n^{\alpha, \beta}(\mathbf{r})} [n_{\text{TF}}^\alpha, n_{\text{TF}}^\beta], \quad (7)$$

gives a good account of the qualitative behavior of the dynamics within the dot, including self-consistent effects associated with the Coulomb interactions. We can therefore use H_{TF} to assess the degree of chaoticity of the dots as well as the effectiveness of the time-reversal breaking term. Figure 1 displays the cumulative density of the nearest-neighbor level spacing for the effective Thomas-Fermi Hamiltonian and for two values of the magnetic field $B=0$ and $B=0.15$ T. (The latter corresponds to about 7 flux quanta through the area of the dot, or a filling factor of about 50 at $r_s \sim 1.4$.) The perfect agreement with the random matrix theory prediction for the Gaussian orthogonal (GOE) or unitary (GUE) ensembles, respectively, shows both that the systems we consider are indeed chaotic and that $B=0.15$ T is enough to break time-reversal invariance. We have performed additional checks on the statistics of the wave functions, and in particular on the distribution of the quantities M_{ij} and N_{ij} introduced in Eq. (9), which further confirms this point.

Being confident that the choice of parameters and magnetic field corresponds to the regime we would like to study, we can now compute the ground-state energy and spin for our model quantum dot with the full-fledged LSDA self-consistent approach. The resulting distributions of addition energy and ground-state spins, for particle number N in the range [120, 200], are shown in Figs. 2 and 3.

We would like now to compare these distributions with theoretical predictions in which (i) the interactions are treated by a RPA-like approach and (ii) the statistical properties of the eigenlevels and eigenfunctions are modeled in terms of RMT and RPW. The RPA treatment of the interactions^{10,14} is essentially a Landau-Fermi-liquid picture in which the electrons are considered to be quasiparticles

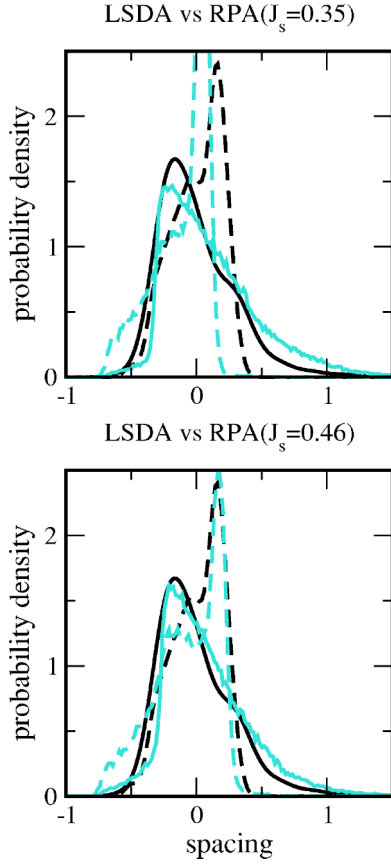
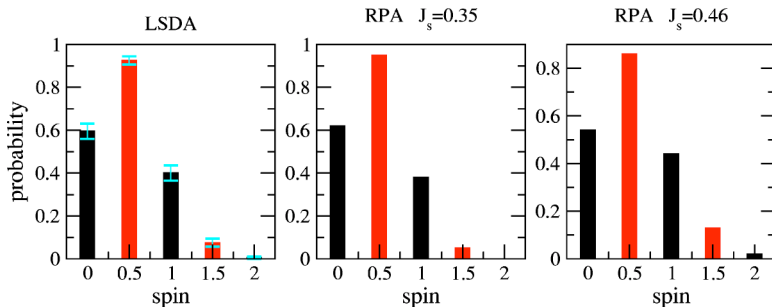


FIG. 2. (Color online) Addition spectra obtained from the LSDA calculations (dark), compared with theoretical predictions derived from RPA/RPW (lighter, blue online). Solid: N even; Dashed: N odd. Top: strength of the RPA interaction obtained by matching the QMC value, $J_s = f_a^0 = 0.35$ (for $r_s = 1.4$). Bottom: better agreement is obtained with a slightly larger value of this parameter, $J_s = 0.46$.

evolving under an effective one-particle Hamiltonian H_{eff} (which we can think of as being H_{TF}) and interacting through a weak short-range residual interaction $V_{\text{RPA}}(\mathbf{r} - \mathbf{r}')$. For *broken time-reversal symmetry*, $V_{\text{RPA}}(\mathbf{r} - \mathbf{r}')$ can be taken into account by first-order perturbation theory. Up to a smooth component in which we are not interested, the energy of the quantum dot for a given set of occupation numbers $f_i^\sigma = 0, 1$ of the orbitals ψ_i of H_{eff} is therefore the sum of the one-particle energies

$$E_{1p} = \sum f_i^\sigma \epsilon_i \quad (8)$$

and the residual interaction direct plus exchange terms



$$E_{ii} = \frac{1}{2} \sum_{i,j,\sigma,\sigma'} f_i^\sigma f_j^{\sigma'} M_{ij} - \frac{1}{2} \sum_{i,j,\sigma} f_i^\sigma f_j^\sigma N_{ij}, \quad (9)$$

with

$$M_{ij} = \int d\mathbf{r} d\mathbf{r}' |\psi_i(\mathbf{r})|^2 V_{\text{RPA}}(\mathbf{r} - \mathbf{r}') |\psi_j(\mathbf{r}')|^2,$$

$$N_{ij} = \int d\mathbf{r} d\mathbf{r}' \psi_i(\mathbf{r}) \psi_j^*(\mathbf{r}) V_{\text{RPA}}(\mathbf{r} - \mathbf{r}') \psi_j(\mathbf{r}') \psi_i^*(\mathbf{r}').$$

Note that once the interaction potential $V_{\text{RPA}}(\mathbf{r} - \mathbf{r}')$ is determined, all the relevant quantities are expressed in terms of the eigenvalues ϵ_i and eigenfunctions ψ_i of H_{eff} . The RMT/RPW model consists of fixing the eigenvalue fluctuations according to RMT and those of the eigenfunctions by describing them as a superposition of random plane waves, for levels within the Thouless energy of the Fermi energy. This fixes the fluctuations of E_{1p} and of the M_{ij} and N_{ij} .

The weak interaction obtained from the RPA treatment^{10,14} is quite naturally the zero frequency and low-momentum approximation of the screened RPA interaction, which for 2D systems takes the form

$$V_{\text{RPA}}^0(\mathbf{r}) = \int \frac{d\mathbf{q}}{(2\pi)^2} \hat{V}_{\text{RPA}}^0(\mathbf{q}) \exp[i\mathbf{q} \cdot \mathbf{r}],$$

$$\hat{V}_{\text{RPA}}^0(\mathbf{q}) = \frac{N(0)^{-1}}{1 + r_s^{-1}(|\mathbf{q}|/k_F)/\sqrt{2}}. \quad (10)$$

It is known from quantum Monte Carlo (QMC) results that, in the regime of interest, RPA slightly underestimates the interaction strength. Thus we use a boosted interaction

$$V_{\text{RPA}} = \xi V_{\text{RPA}}^0(\mathbf{r}) \quad (11)$$

with ξ adjusted so that RPA matches QMC. Note that this is completely consistent since the Tanatar-Ceperley parametrization of LSDA comes from fitting the QMC results as well. The natural quantity to match is the Fermi circle average

$$J_S \equiv \langle \hat{V}_{\text{RPA}} \rangle_{\text{fs}} = \int_0^{2\pi} \frac{d\theta}{2\pi} \hat{V}_{\text{RPA}}(k_F \sqrt{2(1 + \cos \theta)}), \quad (12)$$

which should be interpreted as the Fermi-liquid parameter f_a^0 . For the value $r_s = 1.4$ considered here, QMC gives (Ref. 21) $f_a^0 = 0.35$ while $\langle \hat{V}_{\text{RPA}} \rangle_{\text{fs}} = 0.31$. Thus, for our density, the natural value is $\xi = 1.1$; we have used other values as well in order to explore trends.

FIG. 3. (Color online) Spin distribution obtained from the LSDA calculations (left), the RPA/RPW model with $J_s = f_a^0 = 0.35$ (middle), and $J_s = 0.46$ (right). Contrary to the addition spectra, slightly enhancing the RPA interaction does not improve the agreement with the LSDA simulation for the spin distribution; rather, it makes it worse.

The distributions of addition energy and ground-state spin for $\xi=1.1$ and 1.5 , corresponding to $J_s=0.35$ ($=J_a^0$) and 0.46 , are shown in Figs. 2 and 3. We observe that, although the lower value of the interaction gives already reasonable agreement for the addition energy distribution, a better result is obtained, especially for N odd, when the interaction is enhanced. In contrast, the spin distribution is accurately reproduced by just taking $J_s=f_0^a$, while the stronger interaction predicts slightly too many high spin ground states.

Despite the apparent contrast here, these results are nicely in line with the analysis using the Strutinsky approximation in Ref. 15. Indeed, the results there indicate that the main source of discrepancy between LSDA and RPA/RPW comes from the absence of screening of the Cooper channel in the former. *Since the Cooper channel does not contribute when time-reversal symmetry is broken, the much better agreement between LSDA and RPA/RPW here, as compared to the time-reversal invariant situation considered before,^{8,15} demonstrates the importance of this higher-order interaction effect in the ground-state properties of quantum dots.*

It was also pointed out in Ref. 15 that beyond the effect of the Cooper channel, LSDA differed from RPA/RPW in two aspects: (i) a slightly larger effective residual interaction and (ii) the existence of spin contamination, i.e., of solutions of the Kohn-Sham equations with different wave functions for the majority and minority spins. The first of these points explains why it is necessary to slightly enhance the RPA interaction to perfectly reproduce the LSDA addition energy distribution. The spin contamination mechanism, however,

has a tendency to produce slightly smaller ground-state spins, and therefore offsets the first point when the statistics of spin ground states are considered. As a consequence, spin statistics from the LSDA calculations nicely agree with the RPA/RPW prediction without enhancing the RPA interaction.

To conclude, we have shown that because of the absence of the Cooper channel contribution when time-reversal symmetry is broken, the addition energy and ground-state spin statistics obtained from LSDA calculations for a chaotic quartic oscillator at weak magnetic field closely follow RPA/RPW predictions. This demonstrates in an unambiguous way that higher-order interaction effects in the Cooper channel are indeed the main cause of the discrepancies observed between LSDA and RPA/RPW in the time-reversal symmetric case. The remaining differences can be understood as arising from a combination of spin contamination and the slightly larger effective interaction that can be derived from LSDA within a second-order Strutinsky scheme. Finally, we stress that beyond these differences, both methods predict a great sensitivity of the addition energy distribution (at weak magnetic field) to the precise value of the exchange parameter J_s . We suggest that experimentally measuring these distributions, at a temperature low enough¹² to resolve the shift in the maxima between the odd and even distributions, would provide a sensitive way to directly access this quantity.

This work was supported in part by NSF Grant No. DMR-0103003.

*Permanent address: Laboratoire de Physique Théorique et Modèles Statistiques (LPTMS), 91405 Orsay Cedex, France.

†Present address: Institut für Theoretische Physik, J. W. Goethe-Universität, Frankfurt am Main, Germany.

¹L. P. Kouwenhoven, C. M. Marcus, P. L. McEuen, S. Tarucha, R. M. Wehrl, and N. S. Wingreen, in *Mesoscopic Electron Transport*, edited by L. L. Sohn, G. Schön, and L. P. Kouwenhoven (Kluwer, Dordrecht, 1997), pp. 105–214.

²R. M. Potok, J. A. Folk, C. M. Marcus, V. Umansky, M. Hanson, and A. C. Gossard, *Phys. Rev. Lett.* **91**, 016802 (2003).

³E. Buks, R. Schuster, M. Heiblum, D. Mahalu, and V. Umansky, *Nature (London)* **391**, 871 (1998).

⁴T. Hayashi, T. Fujisawa, H. D. Cheong, Y. H. Jeong, and Y. Hirayama, *Phys. Rev. Lett.* **91**, 226804 (2003).

⁵R. G. Parr and W. Yang, *Density-Functional Theory of Atoms and Molecules* (Oxford University Press, New York, 1989).

⁶R. O. Jones and O. Gunnarsson, *Rev. Mod. Phys.* **61**, 689 (1989).

⁷S. M. Reimann and M. Manninen, *Rev. Mod. Phys.* **74**, 1283 (2002), and references therein.

⁸H. Jiang, H. U. Baranger, and W. Yang, *Phys. Rev. Lett.* **90**, 026806 (2003).

⁹H. Jiang, D. Ullmo, W. Yang, and H. U. Baranger, *Phys. Rev. B* **69**, 235326 (2004).

¹⁰Y. M. Blanter, A. D. Mirlin, and B. A. Muzykantskii, *Phys. Rev. Lett.* **78**, 2449 (1997).

¹¹D. Ullmo and H. U. Baranger, *Phys. Rev. B* **64**, 245324 (2001).

¹²G. Usaj and H. U. Baranger, *Phys. Rev. B* **64**, 201319(R) (2001).

¹³G. Usaj and H. U. Baranger, *Phys. Rev. B* **66**, 155333 (2002), and references therein.

¹⁴I. L. Aleiner, P. W. Brouwer, and L. I. Glazman, *Phys. Rep.* **358**, 309 (2002), and references therein.

¹⁵D. Ullmo, H. Jiang, W. Yang, and H. U. Baranger, *Phys. Rev. B* **70**, 205309 (2004).

¹⁶For a discussion of the Cooper channel in the context of ballistic quantum dots, see, e.g., D. Ullmo, H. U. Baranger, K. Richter, F. von Oppen, and R. A. Jalabert, *Phys. Rev. Lett.* **80**, 895 (1998), and references therein, for diffusive systems.

¹⁷B. Tanatar and D. M. Ceperley, *Phys. Rev. B* **39**, 5005 (1989).

¹⁸The current dependence of the exchange-correlation energy functional, which plays a critical role in the quantum Hall regime, is neglected in this work since we are interested in only the low magnetic-field regime [see, e.g., M. Ferconi and G. Vignale, *Phys. Rev. B* **50**, 14722 (1994)].

¹⁹H. Jiang, H. U. Baranger, and W. Yang, *Phys. Rev. B* **68**, 165337 (2003).

²⁰H. Jiang and W. Yang, *J. Chem. Phys.* **121**, 2030 (2004).

²¹More precisely, this value corresponds to the parametrization of the exchange-correlation functional we have used in the LSDA calculations.